ACS OMEGA

http://pubs.acs.org/journal/acsodf

Article

# Effect of Prestirring Time on Carbon Removal from Coal Fly Ash in the Flotation Technology

Ke Liu, Jinming Jiang,* Koji Takasu,* Jian Wan, and Weijun Gao

Cite This: *ACS Omega* 2023, 8, 27794−27801

Read Online

ACCESS | Metrics & More | Article Recommendations

**ABSTRACT:** Coal fly ash (CFA) is one of the industrial byproducts of burning coal for energy production and has unburned carbon, which negatively affects its full potential use. The flotation technology can be effective in separating unburned carbon from CFA, and the prestirring time is crucial for the ideal initial conditions during the flotation process. To find the suitable prestirring time, eight prestirring times, including 0, 1, 2, 3, 4, 5, 6, and 7 min, were selected in this paper, followed by flotation of CFA after prestirring. Parameters such as loss on ignition (LOI), the removal rate of unburned carbon (RUC), contact angle, and particle size volume fraction were used to assess the effect of prestirring time on flotation results. The results showed that the prestirring time significantly affects the CFA flotation performance. As the prestirring time increased, the LOI of CFA first decreased and then increased, and the contact angle showed the opposite trend. Besides, the prestirring time of over 2 min positively affected the fineness of the tailings. Overall, the prestirring time of 3 min had the most significant carbon removal effect, obtaining an LOI of tailings of 0.96%, a yield of 74.56%, an RUC of 72.70%, and a volume fraction less than 45 $\mu$m of 36.65%. This study provides theoretical support for improving stirring efficiency and saving flotation costs in industrial applications and is conducive to the recycling of CFA resources.

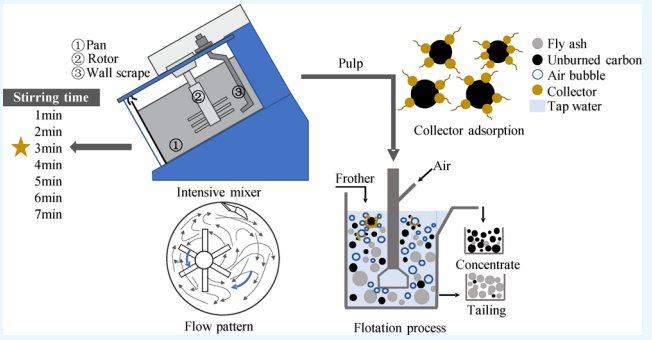


## 1. INTRODUCTION

Coal fly ash (CFA) is among the greatest sources of fuel waste residues, with the coal industry worldwide producing approximately 750 million tons annually.[1] However, the real amount of CFA reused is still less than the amount created, with a utilization ratio of just 30%.[2] The unburned carbon percentage of CFA has generally ranged between 2 and 12%. Moreover, unburned carbon impedes the utilization or effective use of CFA, especially within the building materials industry.[3] The actual percentage of unburned carbon use restrictions varies among regulatory agencies. In accordance with the Chinese national standard GB/T 1596−2017 (Fly Ash Used for Cement and Concrete), the loss on ignition (LOI) of grade I fly ash should be less than 5% and even less than 3% in the construction industry. In addition, the carbon enriched in CFA can be utilized as coke in the metallurgical industry,[4] as a precursor for activated carbon preparation[5] or as graphite-like materials.[6] Compared with landfill disposal or storage, reutilizing separated CFA and unburned carbon can reduce energy consumption and achieve greater environmental benefits.

Unburned carbon can be segregated from CFA for beneficial reuse by sieving,[7] gravity separation,[8] electrostatic separation,[9] froth flotation,[10] acid digestion, and sink-float technique (density separation).[11] At present, froth flotation is commonly used as a separation technique in the concentrating and coal beneficiation industries, relying on the capability of the bubbles to cling to the surface of specific particles in a selective manner. However, the burning of coal at high temperatures results in the formation of porous and highly oxidized surfaces of unburned carbon, as well as some difficult-to-float minerals melted onto the unburned carbon surface throughout the burning process.[12] Therefore, the unburned carbon removal process has the technical problem of poor floatability compared to the flotation of minerals.

Pulp stirring is the starting point of flotation, and therefore, pulp conditioning is extremely important in the flotation system as a pretreatment before flotation.[13] Due to its significant impact on the mixing, conveying, and reaction phenomena that are occurring, as well as on kinetic energy consumption and operational efficiencies, stirring is crucial for a majority of process performance aspects.[14] Consequently, pulp stirring is crucial for the suspension and stirring of particles, dispersion of

Received: June 10, 2023
Accepted: July 12, 2023
Published: July 23, 2023

Table 1. X-ray Fluorescence Analysis Results of the CFA Sample

| components | $SiO_2$ | $Al_2O_3$ | $Fe_2O_3$ | CaO | $SO_3$ | $TiO_2$ | $K_2O$ | $Na_2O$ |
|---|---|---|---|---|---|---|---|---|
| content (%) | 49.72 | 34.17 | 7.14 | 3.15 | 1.41 | 1.32 | 1.29 | 0.64 |
| components | MgO | $P_2O_5$ | MnO | SrO | $ZrO_2$ | Cl | $Co_3O_4$ | $Cr_2O_3$ |
| content (%) | 0.62 | 0.25 | 0.07 | 0.06 | 0.04 | 0.03 | 0.02 | 0.02 |

agents in the pulp, uniform stirring and collision of agents and particles, and effective adsorption.[15] Although some articles have emphasized the influence of preconditioning on CFA flotation, most have focused on the study of the impact of prestirring speed on the flotation process.[16,17] However, prestirring time is one of the most critical parameters of the stirring operation, which is also among the major variables impacting the flotation results.[18] Song et al.[19] indicated that prestirring time with a fixed stirring strength controlled the amount of kinetic energy input. The amount of energy input during prestirring could significantly impact pulp-stirring efficiency and subsequent flotation performance.[20] Chang et al.[21] investigated the impact of prestirring duration on froth flotation's ability to remove graphene oxide. Analysis indicated that the removal increased as prestirring time increased, demonstrating the need for sufficient energy input to achieve aggregation and flotation separation. Yang et al.[22] noted that prestirring time significantly influenced the degree of agglomeration and the morphology of aggregates in apatite fines during flotation. When the prestirring speed was 1300 rpm, a certain extension of the prestirring time led to a reduction in the agglomeration and more regular agglomerates. Jin et al.[23] investigated hydrophobic flocculation flotation of scheelite and cassiterite under NaOL and BHA systems. They concluded that the prestirring time and prestirring speed could improve the flotation rate, recovery, and aggregate size. Besides, several studies have investigated the impact of prestirring time on the results of flotation of rutile fines,[18] pyrites,[24] and ultrafine molybdenites.[25]

Based on the above review, prestirring time significantly affects flotation results. However, most of the research on the impact of prestirring time on the flotation effect is mainly concentrated on mineral flotation, but there are few kinds of research on the effect of CFA flotation. This paper discussed the impact of various prestirring times upon the flotation properties of the CFA. In the prestirring process, an intense mixer was used to prepare the pulp at eight different prestirring times, and flotation experiments were performed to verify the flotation effect. To assess the impact of prestirring time on the separation of unburnt carbon in CFA, a number of parameters, including LOI, the removal rate of unburned carbon (RUC), yield, and contact angle, were measured. Furthermore, the CFA flotation mechanism was discussed with an X-ray photoelectron spectrometer (XPS) and a scanning electron microscopy−energy-dispersive spectrometer (SEM−EDS).

## 2. MATERIALS

The CFA was obtained from the Huaneng Power Plant in Qingdao, Shandong Province, China. The percentage of unburned carbon present in CFA was calculated utilizing the LOI analysis in accordance with the ASTM D7348-13 standard.[26] The LOI of CFA is 8.94%, and the chemical composition analysis is reported in Table 1. X-ray diffraction (XRD, SmartLab SE, Rigaku, Japan) analysis was employed to determine the inorganic mineral content of CFA. The CFA sample was ground to −0.05 mm and the test was carried out at room temperature. The test light source was X-ray tube copper target radiation with a tube voltage of 40 kV, a current of 40 mA, and a scanning range of 0−150°. The XRD result indicated that the main minerals found in CFA were quartz and mullite, accounting for 81.9 and 18.1%, respectively (Figure 1). Kerosene and pine oil were used as the collector and frother, respectively. The water used in the experiment was tap water.

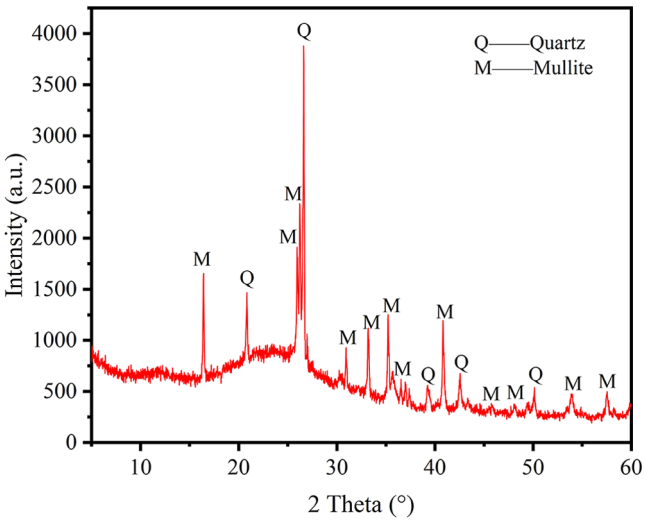


Figure 1. XRD patterns of the CFA sample.

## 3. EXPERIMENTAL METHODS

**3.1. Experimental Process.** The flotation experiments were completed with an XFD-type flotation cell of 1.5 L capacity, and Figure 2 illustrates the procedure. First, 20 kg of CFA, 30% of water, and 2% of the collector were added to the mixer at a rotor speed of 800 rpm and a pan speed of 25 rpm. The prestirring times were set as 0, 1, 2, 3, 4, 5, 6, and 7 min. Then, the pulp collected after prestirring was fed into the flotation cell while the impeller was running at 1800 rpm. Afterward, water and 0.2% frother were added to maintain the pulp concentration at 11%. Finally, the air was delivered to the flotation cell at a flow rate of 2.0 L/min. After 20 min of flotation, the froth product and the pulp product that remained in the flotation cell were processed as concentrates and tailings, respectively.

In particular, the prestirring tests for the preparation of the pulp were carried out in an Erich intensive mixer type R05T. Most of the prestirring of CFA in the available literature was done directly in the Denver flotation cell and was still at the laboratory scale level.[27] However, batch and industrial-scale flotation placed higher demands on stirring efficiency. The stirring equipment used in this study had a diameter of 55 cm, a height of 40 cm, and an effective volume of 40 L. It was demonstrated that prestirring using this type of stirring equipment can result in low LOI tailings,[28] and the rotor rotated in the opposite direction to the mixing pan, enabling the material to form a swirling material flow during the stirring process, as shown in Figure 2. For subsequent flotation


https://doi.org/10.1021/acsomega.3c04121
ACS Omega 2023, 8, 27794−27801

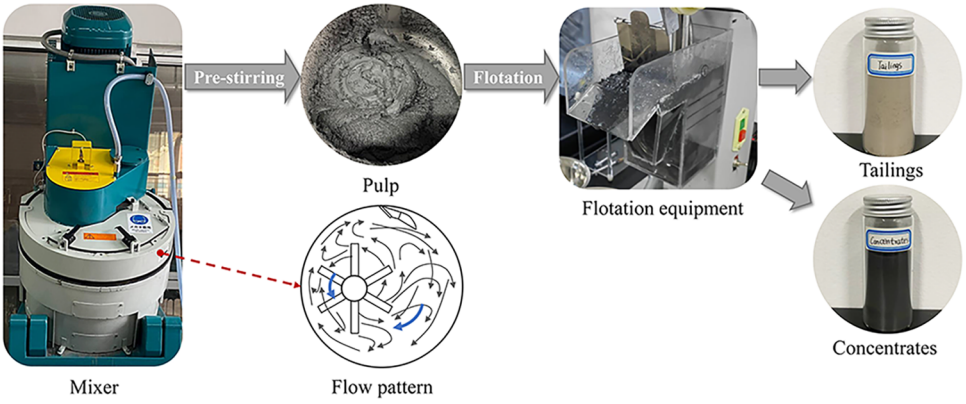


**Figure 2.** Process of flotation experiments.

experiments, the pulp was taken uniformly at four points on two vertical symmetry axes and at the center of the mixer.

**3.2. Evaluation Parameters.** To assess the impact of prestirring time on the CFA flotation performance, several parameters were selected, namely, LOI, RUC, yield, and size volume distribution of the tailings, the contact angle of the pulp, and SEM−EDS and XPS measurements.

*3.2.1. Flotation Result Measurement.* To determine LOI, RUC, and yield, the concentrates and tailings obtained at different prestirring times were filtered, dried, and weighed. The following formula was used to compute the LOI

$$\mathrm{LOI}\ (\%) = \frac{W_b - W_a}{W_b} \times 100 \quad (1)$$

where $W_b$ and $W_a$ denote the masses of CFA and post-combustion CFA, respectively. The carbon recoveries from the concentrate were equivalent to RUC, which was calculated as follows

$$\mathrm{RUC}\ (\%) = \frac{\mathrm{LOI}_C \times Y_C}{\mathrm{LOI}_R} \times 100 \quad (2)$$

where $\mathrm{LOI}_C$ and $\mathrm{LOI}_R$ denote the LOI of concentrates and CFA, respectively, and $Y_C$ denotes the yield of the concentrate.

*3.2.2. Contact Angle Analysis.* After prestirring, contact angles of the CFA were determined via a DSA25E (KRUSS, Germany) instrument to determine the hydrophobicity of the CFA surface. The test samples were prepared by taking 1.5 g of pressed slices after drying the CFA and the pulp after different prestirring times. Subsequently, the samples were placed on the carrier table, and 1 $\mu$L of deionized water was squeezed out with a microsyringe to keep the droplets on the surface of the samples, and then the images were frozen. The contact angle value was measured by the goniometric method to compare and analyze the improvement of hydrophobicity of CFA at various prestirring times.

*3.2.3. Particle Size Distribution Measurement.* The particle size analysis of CFA and tailings was conducted using a Mastersizer 2000 (Malvern, England) laser particle size analyzer. The solution sample was prepared using water as a solvent for wet testing. When the laser beam traveled through the dispersed CFA sample particulate, the size of the CFA particles was determined through measurement of the scattered light intensity.

*3.2.4. SEM−EDS Analysis.* A SIGMA 300 (Carl Zeiss, Germany) scanning electron microscope and an energy-dispersive spectrometer were used for the analysis of the surface morphology and elemental localization of the CFA, concentrates, and tailings gathered in the experiment. Prior to the measurement, the sample was coated with gold to prepare the final test sample. Then, the sample was scanned in a lower vacuum setting. The SEM's precise operating settings were as follows: EHT = 10.00 kV, WD = 6.7 mm, and signal = Inlens. Additionally, in each measurement, two or four locations on the sample surface were chosen for energy-dispersive spectroscopy evaluation of the elemental composition of the sample.

*3.2.5. XPS Analysis.* By employing an X-ray photoelectron spectrometer (Thermo Fisher Scientific K-Alphah) in an ultrahigh vacuum system, the elemental components and content of the samples were measured. Wide scan testing at 1 eV step energy was carried out to determine the concentrations of carbon, oxygen, silicon, aluminum, and other components. After drying and grinding, CFA, the concentrate, and tailings (about 0.2 g) were analyzed.

## 4. RESULTS AND DISCUSSION

**4.1. Flotation Test Results.** The LOI, yield, and RUC of CFA at different prestirring times are presented in Figure 3. As

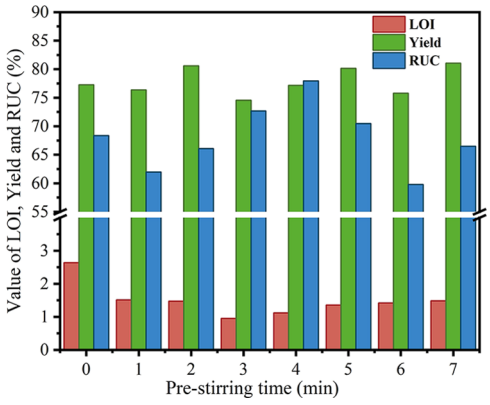


**Figure 3.** Flotation results at different prestirring times.

the prestirring time increased during flotation, the LOI of the tailings dropped significantly at the beginning and then reached a minimum at about 3 min. Afterward, it increased marginally with the extended prestirring time, while RUC showed the opposite trend. With the prestirring time going from 0 to 1 min, the LOI dropped from 2.64 to 1.31%. The LOI decreased to 0.96% and the RUC increased from 61.97 to 72.70% as the prestirring time was extended to 3 min. The prestirring time



https://doi.org/10.1021/acsomega.3c04121
ACS Omega 2023, 8, 27794−27801

increased further to 7 min, with a slight increase in LOI and a gradual decrease in RUC. Besides, the tailings yield varied nonlinearly with the prestirring time. The differences in tailings yield were within 6.50% when the prestirring time ranged from 0 to 7 min. The suitable prestirring time was 3 min, and the LOI, tailings yield, and RUC were 9.56, 74.56, and 72.70%, respectively. It is obvious that prestirring time has a big impact on CFA flotation. In terms of mixing uniformity, low prestirring time leads to insufficient mixing, which does not ensure particle dispersion and collector emulsification, affecting the collision and absorption efficiency of particles and the collector, and reducing the floatability of CFA. The degree of mixing gradually increases with the prestirring time until it reaches the highest uniformity, which is called the dynamic equilibrium. If the prestirring time continues to be prolonged, the pulp tends to separate with droplets floating up and particles sinking down. So that the mixing uniformity is reduced, which is called overmixing. Therefore, the pulp should be discharged from the stirring device when the optimum mixing condition is obtained.[29] Considering the aspect of particle agglomeration, the formation and breakage of the agglomerate occur at the same time during hydrophobic agglomeration.[30] The prestirring process provides energy to bring the particles close to each other to form agglomerates, diffusing oil droplets from the surface of the hydrophobic to the oil bridge among the particles and enhancing the floatability on the surface of the particles. However, excessive prestirring will cause the rupture of agglomerates, which adversely affects the CFA flotation results.[22]

**4.2. Contact Angle Analysis.** In the mineral processing sector, the contact angle represents a crucial characteristic to reflect the hydrophobicity of particles. Figure 4 shows the CFA

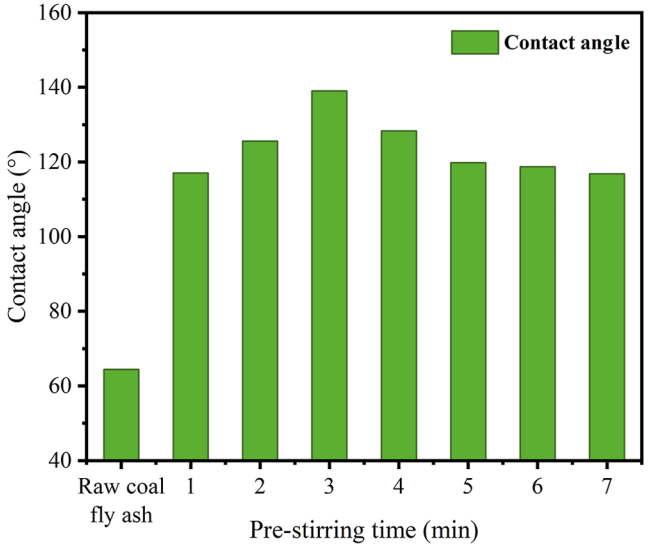


**Figure 4.** Contact angle of samples at different prestirring times.

contact angle information at various premixing times. As well, Figure 5 shows the contact states of CFA and deionized water. As shown in Figures 4 and 5, the contact state changed with the extension of prestirring time, and the contact angle first increased and then decreased. The untreated CFA sample has a contact angle of 64.4°, which is in a hydrophilic state (less than 90°). Because the surface of char particles contained a lot of hydrophilic oxygen-containing functional groups after high-temperature oxidation in the furnace, their contact angle was greatly reduced, indicating that the unburned carbon of the CFA had a poor capacity to float. Unburned carbon particles had a greater contact angle after prestirring with the collector. The contact angle increased from 117.0 to 139.0° with increasing prestirring time from 1 to 3 min and then it gradually decreased as the prestirring time increased further. It was clear that the contact angle of unburned carbon for 3 min of prestirring time was the largest, indicating that the hydrophobicity of the surface of unburned carbon particles was the strongest. Therefore, for the same flotation time, prestirring for 3 min is the most effective way to remove carbon from CFA. According to the findings above, prestirring promoted the combination between CFA particles and the collector. Within a suitable prestirring time, the collector, which is broken into oil droplets, gradually mixes well with the CFA particles, increasing the contact angle and hydrophobicity of the unburned carbon particles. As well, friction or shear forces produced when two particles or fluid components move at various speeds cause fine impurities to separate from the particle surface, exposing the natural hydrophobic portion of the unburned carbon. Moreover, the collector molecules precisely prefer to associate with the hydrophobic surface, further enhancing the hydrophobicity of the surface.[16] The results of the flotation test were well supported by the contact angle tests, which demonstrated that the hydrophilic property of the unburnt carbon in CFA could be improved by prestirring.

**4.3. Particle Size Distribution Analysis.** The CFA fineness index was adopted at 45 $\mu$m in accordance with the Chinese national standard GB/T 1596−2017 (Fly Ash Used for Cement and Concrete). Figure 6 shows the distribution curves of tailings particle size and the volume percentage of particle sizes smaller than 45 $\mu$m at different prestirring times. As can be seen, CFA particle size distribution varied at different prestirring times, but the shape of the distribution curve was basically the same. Besides, the volume fraction of tailings < 45 $\mu$m was basically the same as that of the CFA when the prestirring time was 0, 1, and 2 min. When the prestirring time exceeded 2 min, the volume fraction in tailings <45 $\mu$m increased, indicating an increase in the fineness of tailings. As well, by properly increasing the prestirring time, the volume fraction of tailings with particle size <45 $\mu$m can be increased by 10.64% compared to the CFA. At a suitable prestirring time of 3 min, the content of particles <45 $\mu$m increased from 27.40 to 36.65%. Ref 19 presented that when the stirring intensity was fixed, the kinetic energy input was determined by the prestirring time. The extended prestirring time increased the energy input in the preconditioning. In addition, prestirring caused shear damage to the CFA particles by the action of the impeller, the large particles were shredded, and, therefore, more fine particles migrated into the flotation tailings, thus increasing the fineness of the tailings. A study has shown that the finer the CFA particles, the greater the compression resistance and durability of concrete, which positively impacts the application of CFA in construction.[31]

**4.4. Microstructure and Element Analysis.** In order to further verify the separation performance of prestirring preconditioning in the flotation test, the microscopic morphology and component of CFA, concentrate, and tailings at a suitable prestirring time of 3 min were determined, as presented in Figure 7. Figure 7a shows a significant number of irregularly shaped ash particles and a few lumpy carbon skeletons scattered throughout the CFA, suggesting that part of the carbon in the sample was not completely burnt. According to EDS analysis, Si


https://doi.org/10.1021/acsomega.3c04121
ACS Omega 2023, 8, 27794−27801

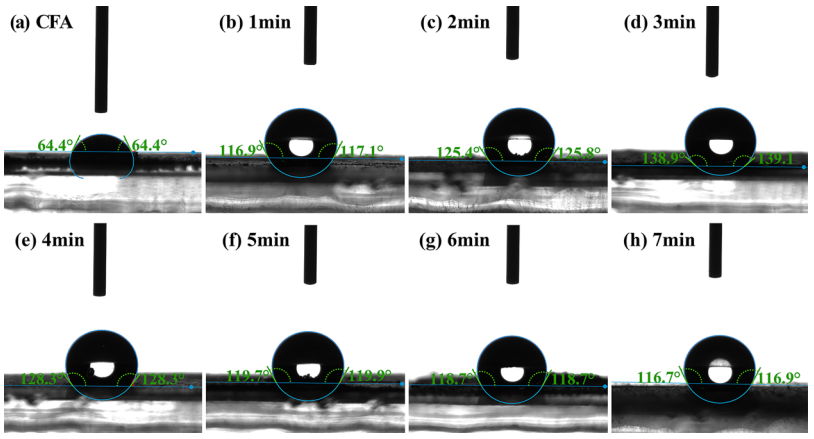


**Figure 5.** Contact angle images of the samples.

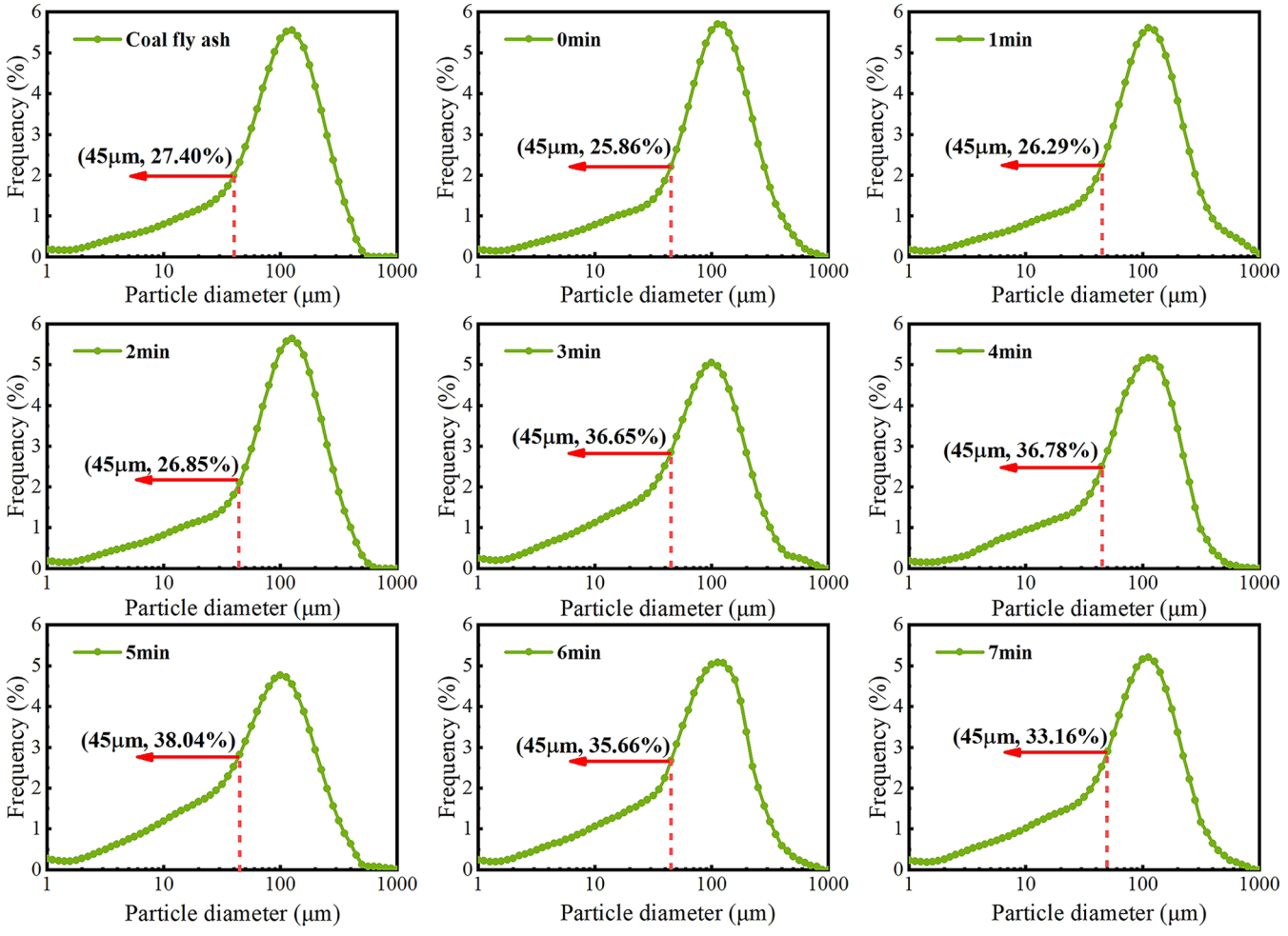


**Figure 6.** Particle size distribution of samples with different prestirring times.

and Al were the main components of the CFA, which was consistent with the outcomes of XRF testing (Table 1). Massive carbon particles and spongy porous structures were obtained in the concentrate, as shown in Figure 7b. The inclusion of tiny glass balls in the unburned carbon particles can be used to explain why there is ash in the concentrate. In addition, the EDS result showed that C was the predominant component of the concentrate at 85.47%. According to Figure 7c, the surface morphology of the flotation tailings and the flotation concentrate differed significantly, with hollow microbeads of varying sizes and a predominant composition of quartz and alumina. Moreover, the EDS result demonstrated that the main components in tailings were O, Al, and Si. The SEM−EDS results confirmed the positive effect of the prestirring procedure on the unburned carbon removal from CFA.

**4.5. Surface Chemical Characteristics Analysis.** By applying XPS measurement, the surface chemical characteristics were examined for tailings, concentrates, and CFA collected at a suitable prestirring time of 3 min, as shown in Figure 8. The findings indicated that there were significant differences in the



https://doi.org/10.1021/acsomega.3c04121
ACS Omega 2023, 8, 27794−27801

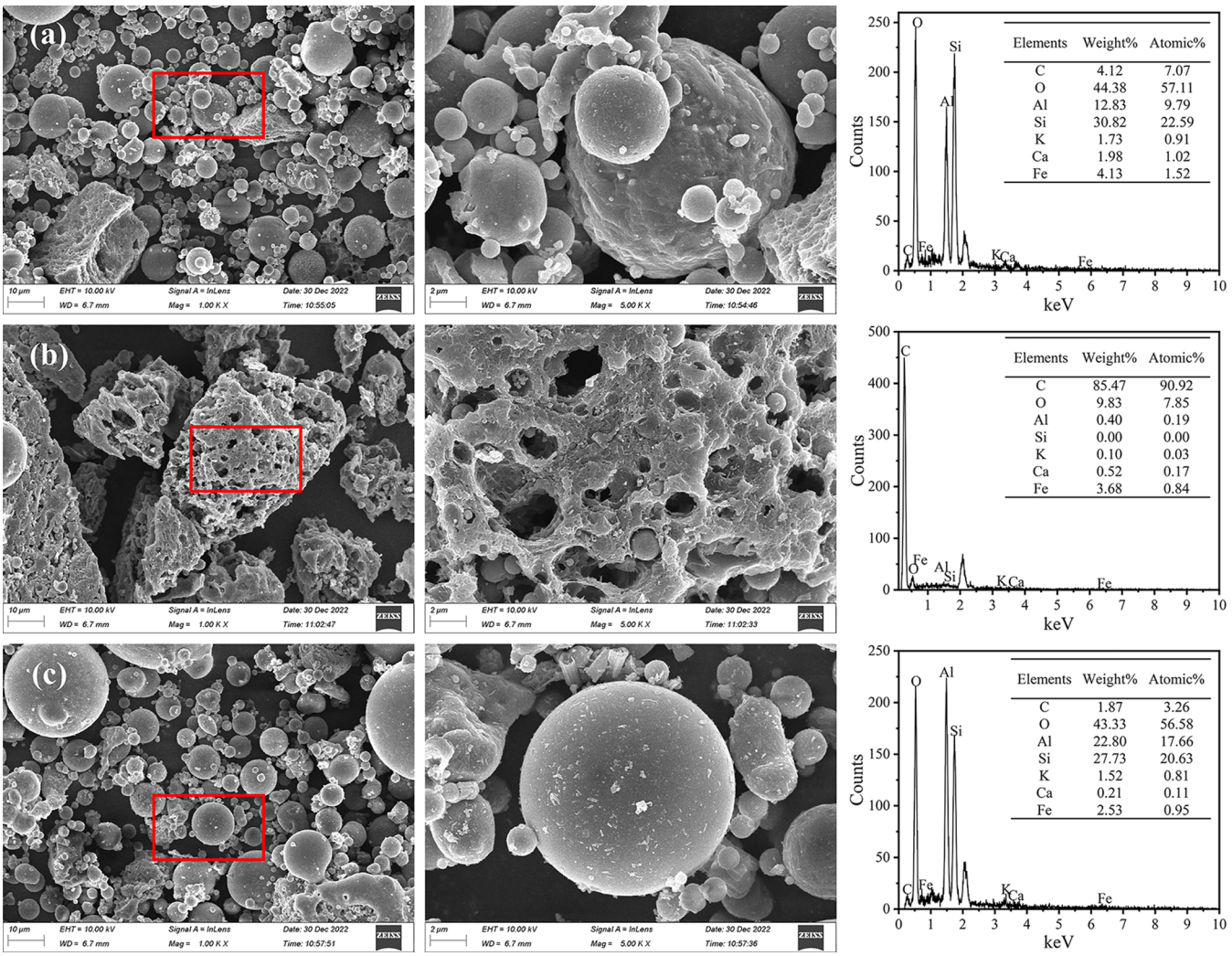


**Figure 7.** SEM−EDS images of (a) CFA, (b) concentrates, and (c) tailings.

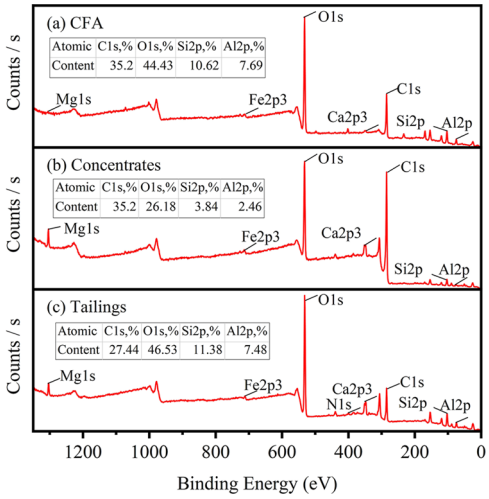


**Figure 8.** XPS spectra of (a) CFA, (b) concentrates, and (c) tailings.

component content of the measured samples, and the blind energies corresponding to the C 1s peaks in CFA, concentrate, and tailings were all 285.08 eV. The C 1s content in the concentrates considerably increased from 35.20 to 61.78% compared to the CFA, and except for O 1s, the C 1s content was much greater than the rest of the components. The C 1s content on the surface of the tailings was the smallest at 27.44%. Moreover, the tailings had higher contents of O 1s, Si 2p, and Al 2p at 46.53, 11.38, and 7.48%, respectively, resulting in high hydrophilicity. The results of XPS analysis and SEM−-EDS analysis were consistent, indicating that flotation at a suitable prestirring time can enhance the separating effectiveness of unburned carbon within CFA, leading to high-quality concentrates and tailings.

## 5. CONCLUSIONS

In this paper, flotation tests were carried out on eight groups of CFA with prestirring times of 0, 1, 2, 3, 4, 5, 6, and 7 min. The main conclusions could be gained as follows:

(1) The LOI of tailings first decreased and then increased as the prestirring time extended. At the most suitable prestirring time of 3 min, the LOI of tailings was 0.96%, RUC was 72.70%, and yield was 74.56%. As well, the CFA and collector reached the optimum mixing state and the CFA achieved the best carbon removal effect. Exceeding the suitable prestirring time not only negatively affects the floatability of the CFA but also increases the cost of the stirring operation in industrial practice.



https://doi.org/10.1021/acsomega.3c04121
ACS Omega 2023, 8, 27794−27801

(2) As the prestirring time extended, the contact angle first increased and then decreased. The contact angle of CFA increased from 64.4 to 139.0° at 3 min of prestirring time, indicating that prestirring enhanced the hydrophobicity of the CFA surface.

(3) Prestirring for more than 2 min increases the fineness of tailings. After 3 min of prestirring, the volume of tailings particle size < 45 $\mu$m increased by 9.25% and the volume of tailings particle size < 100 $\mu$m increased by 11.16% compared to the CFA.

(4) The main components in the concentrate were C and in the tailings were Al and Si, and the C 1s ratio on the surface of the concentrate was as high as 61.78%, which was greater than the C 1s peak intensity in both tailings and CFA. The unburned carbon separation properties from CFA were shown to be significantly enhanced by prestirring.

## AUTHOR INFORMATION


### Corresponding Authors

**Jinming Jiang** − *Faculty of Environmental Engineering, The University of Kitakyushu, Kitakyushu, Fukuoka 8080135, Japan; Innovation Institute for Sustainable Maritime Architecture Research and Technology (iSMART), Qingdao University of Technology, Qingdao 266033, China;* orcid.org/0000-0001-8204-977X; Email: jjmwolf@outlook.com

**Koji Takasu** − *Faculty of Environmental Engineering, The University of Kitakyushu, Kitakyushu, Fukuoka 8080135, Japan; Innovation Institute for Sustainable Maritime Architecture Research and Technology (iSMART), Qingdao University of Technology, Qingdao 266033, China;* Email: takasu@kitakyu-u.ac.jp

### Authors

**Ke Liu** − *Faculty of Environmental Engineering, The University of Kitakyushu, Kitakyushu, Fukuoka 8080135, Japan; Innovation Institute for Sustainable Maritime Architecture Research and Technology (iSMART), Qingdao University of Technology, Qingdao 266033, China*

**Jian Wan** − *Innovation Institute for Sustainable Maritime Architecture Research and Technology (iSMART), Qingdao University of Technology, Qingdao 266033, China*

**Weijun Gao** − *Faculty of Environmental Engineering, The University of Kitakyushu, Kitakyushu, Fukuoka 8080135, Japan; Innovation Institute for Sustainable Maritime Architecture Research and Technology (iSMART), Qingdao University of Technology, Qingdao 266033, China*

Complete contact information is available at: https://pubs.acs.org/10.1021/acsomega.3c04121


### Notes

The authors declare no competing financial interest.

## ACKNOWLEDGMENTS

The authors thank the editor and the anonymous reviewers for their useful feedback that improved this paper. This research did not receive any specific grant from funding agencies in the public, commercial, or not-for-profit sectors.

## REFERENCES


(1) Xing, Y.; Guo, F.; Xu, M.; Gui, X.; Li, H.; Li, G.; Xia, Y.; Han, H. Separation of unburned carbon from coal fly ash: A review. *Powder Technol.* **2019**, *353*, 372−384.

(2) Grabias-Blicharz, E.; Franus, W. A critical review on mechanochemical processing of fly ash and fly ash-derived materials. *Sci. Total Environ.* **2023**, *860*, No. 160529.

(3) Hower, J. C.; Groppo, J. G.; Graham, U. M.; Ward, C. R.; Kostova, I. J.; Maroto-Valer, M. M.; Dai, S. Coal-derived unburned carbons in fly ash: A review. *Int. J. Coal Geol.* **2017**, *179*, 11−27.

(4) Zhao, J.; Liu, H.; Zhang, H.; Song, X.; Zuo, H.; Wang, G.; Xu, Z.; Wu, M.; Zhang, Z.; Chi, R. a. Metallurgical performance and structural characteristics of cokes of hypercoal prepared from the mixture of low-rank coal and biomass residue. *Fuel* **2023**, *332*, No. 126069.

(5) Bartoňová, L. Unburned carbon from coal combustion ash: An overview. *Fuel Process. Technol.* **2015**, *134*, 136−158.

(6) (a) Cabielles, M.; Rouzaud, J.-N.; Garcia, A. B. High-Resolution Transmission Electron Microscopy Studies of Graphite Materials Prepared by High-Temperature Treatment of Unburned Carbon Concentrates from Combustion Fly Ashes. *Energy Fuels* **2009**, *23*, 942−950. (b) Cameán, I.; Garcia, A. B. Graphite materials prepared by HTT of unburned carbon from coal combustion fly ashes: Performance as anodes in lithium-ion batteries. *J. Power Sources* **2011**, *196*, 4816−4820.

(7) De Boom, A.; Degrez, M. Combining sieving and washing, a way to treat MSWI boiler fly ash. *Waste Manage.* **2015**, *39*, 179−188.

(8) Zhang, L.; Yang, F.; Tao, Y. Removal of unburned carbon from fly ash using enhanced gravity separation and the comparison with froth flotation. *Fuel* **2020**, *259*, No. 116282.

(9) Zhou, H.; Chen, Y.; Li, H.; Xu, Z.; Dong, H.; Wang, W. Effect of particles micro characteristics destroyed by ball milling on fly ash electrostatic separation. *Adv. Powder Technol.* **2022**, *33*, No. 103449.

(10) Zheng, K.; Zhang, W.; Li, Y.; Ping, A.; Wu, F.; Xie, G.; Xia, W. Enhancing flotation removal of unburned carbon from fly ash by coal tar-based collector: Experiment and simulation. *Fuel* **2023**, *332*, No. 126023.

(11) Li, C.; Zhou, C.; Li, W.; Zhu, W.; Shi, J.; Liu, G. Enrichment of critical elements from coal fly ash by the combination of physical separations. *Fuel* **2023**, *336*, No. 127156.

(12) Yang, T.; Wang, N.; Gu, H.; Guo, T. Froth flotation separation of carbon from barium slag: Recycling of carbon and minimize the slag. *Waste Manage.* **2021**, *120*, 108−113.

(13) (a) Feng, B.; Feng, Q.; Lu, Y.; Lv, P. The effect of conditioning methods and chain length of xanthate on the flotation of a nickel ore. *Miner. Eng.* **2012**, *39*, 48−50. (b) Li, Z.; Zhao, C.; Zhang, H.; Liu, J.; Yang, C.; Xiong, S. Process intensification of stirred pulp-mixing in flotation. *Chem. Eng. Process. - Process Intensif.* **2019**, *138*, 55−64.

(14) Tabosa, E.; Rubio, J. Flotation of copper sulphides assisted by high intensity conditioning (HIC) and concentrate recirculation. *Miner. Eng.* **2010**, *23*, 1198−1206.

(15) Yang, L.; Zhu, Z.; Qi, X.; Yan, X.; Zhang, H. The Process of the Intensification of Coal Fly Ash Flotation Using a Stirred Tank. *Minerals* **2018**, *8*, 597.

(16) Li, D.; Liang, Y.; Wang, H.; Zhou, R.; Yan, X.; Wang, L.; Zhang, H. Investigation on the effects of fluid intensification based preconditioning process on the decarburization enhancement of fly ash. *Chin. J. Chem. Eng.* **2022**, *44*, 275−283.

(17) Chen, Y.; Zhang, X.; Shi, Q.; Zhang, G.; Li, Q. Investigation of the flotation performance of nickel sulphide by high intensity agitation pretreatment. *Sep. Sci. Technol.* **2022**, *57*, 2955−2959.

(18) Huang, X.-t.; Xiao, W.; Zhao, H.-b.; Cao, P.; Hu, Q.-x.; Qin, W.-q.; Zhang, Y.-s.; Qiu, G.-z.; Wang, J. Hydrophobic flocculation flotation of rutile fines in presence of styryl phosphonic acid. *Trans. Nonferrous Met. Soc. China* **2018**, *28*, 1424−1432.

(19) Song, S.; Lopez-Valdivieso, A.; Reyes-Bahena, J. L.; Bermejo-Perez, H. I.; Trass, O. Hydrophobic Flocculation of Galena Fines in Aqueous Suspensions. *J. Colloid Interface Sci.* **2000**, *227*, 272−281.

(20) (a) Feng, D.; Aldrich, C. Effect of Preconditioning on the Flotation of Coal. *Chem. Eng. Commun.* **2005**, *192*, 972−983. (b) Li, D.; Liang, Y.; Wang, H.; Yang, L.; Yan, X.; Wang, L.; Zhang, H. Effect of

slurry preconditioning on the occurrence of major minerals in the flotation products of coal. *Int. J. Coal Prep. Util.* **2022**, *42*, 2597−2612.
(21) Chang, L.; Cao, Y.; Peng, W.; Li, C.; Fan, G.; Song, X.; Jia, C. Insight into the effect of oxidation degree of graphene oxides on their removal from wastewater via froth flotation. *Chemosphere* **2021**, *262*, No. 127837.
(22) Yang, B.; Huang, P.; Song, S.; Luo, H.; Zhang, Y. Hydrophobic agglomeration of apatite fines induced by sodium oleate in aqueous solutions. *Results Phys.* **2018**, *9*, 970−977.
(23) Jin, S.; Ou, L. Comparison of the Effects of Sodium Oleate and Benzohydroxamic Acid on Fine Scheelite and Cassiterite Hydrophobic Flocculation. *Minerals* **2022**, *12*, 687.
(24) Nikolaev, A. A.; Batkhuyag, A.; Goryachev, B. Mineralization Kinetics of Air Bubble in Pyrite Slurry under Dynamic Conditions. *J. Min. Sci.* **2018**, *54*, 840−844.
(25) Jiangang, F.; Kaida, C.; Hui, W.; Chao, G.; Wei, L. Recovering molybdenite from ultrafine waste tailings by oil agglomerate flotation. *Miner. Eng.* **2012**, *39*, 133−139.
(26) ASTM. *Standard Test Methods for Loss on Ignition (LOI) of Solid Combustion Residues*; West Conshohocken, PA, 2013.
(27) Yang, L.; Li, D.; Zhu, Z.; Xu, M.; Yan, X.; Zhang, H. Effect of the intensification of preconditioning on the separation of unburned carbon from coal fly ash. *Fuel* **2019**, *242*, 174−183.
(28) Lin, H.; Takasu, K.; Suyama, H.; Koyamada, H.; Liu, S. A study on properties, static and dynamic elastic modulus of recycled concrete under the influence of modified fly ash. *Constr. Build. Mater.* **2022**, *347*, No. 128585.
(29) Zhu, C. Inorganic Solidified Foam Generation Device and Experiment Research for Preventing and Controlling Combustion of coal. Doctoral Thesis, China University of Mining and Technology, 2016.
(30) Lu, S.; Ding, Y.; Guo, J. Kinetics of fine particle aggregation in turbulence. *Adv. Colloid Interface Sci.* **1998**, *78*, 197−235.
(31) Assi, L. N.; Eddie Deaver, E.; Ziehl, P. Effect of source and particle size distribution on the mechanical and microstructural properties of fly Ash-Based geopolymer concrete. *Constr. Build. Mater.* **2018**, *167*, 372−380.



https://doi.org/10.1021/acsomega.3c04121
*ACS Omega* 2023, 8, 27794−27801